Eur. Phys. J. D **11**, 473–480 (2000)

The European Physical Journal D

EDP Sciences

Ultra-low-frequency electrostatic and electromagnetic modes in self-gravitating magnetized dusty plasmas

A.A. Mamun[1,a] and A.A. Gebreel[2]

[1] Department of Physics, Jahangirnagar University, Savar, Dhaka, Bangladesh
[2] University of Cambridge, Cavendish Laboratory, Cambridge CB3 OHE, UK

Received 16 December 1999

Abstract. A theoretical investigation has been made of ultra-low-frequency dust-electrostatic and dust-electromagnetic modes, propagating perpendicular to the external magnetic field, in a self-gravitating, warm, magnetized, two fluid dusty plasma system. It has been shown that the effects of self-gravitational field and dust thermal pressure significantly modify the dispersion properties of these ultra-low-frequency dust-modes. It is also found that under certain conditions, the self-gravitational effect can destabilize these ultra-low-frequency dust-electrostatic and dust-electromagnetic modes. However, the effects of the external magnetic field and dust and ion thermal pressures are found to play stabilizing role, *i.e.*, these effects make these modes stable and counter the gravitational condensation of the dust grains. The implications of these results to some space and astrophysical dusty plasma systems, especially, to planetary ring-systems and cometary tails, are briefly mentioned.

PACS. 52.35.Fp Electrostatic waves and oscillations (e.g., ion-acoustic waves) – 52.35.Lv Other linear waves – 52.25.Zb Dusty plasmas; plasma crystals

1 Introduction

Recently, there has been a great deal of interest in understanding wave propagation in dusty plasmas (plasmas with extremely massive and negatively charged dust grains), because of its vital role in the study of astrophysical and space environments, such as, asteroid zones, planetary atmospheres, interstellar media, circumstellar disks, dark molecular clouds, cometary tails, nebulae, earth's environment, etc. [1–7]. These dust grains are invariably immersed in the ambient plasma and radiative background. The interaction of these dust grains with the other plasma particles (*viz.* electrons and ions) is due to the charge carried by them. These dust grains are charged by a number of competing processes, depending upon the local conditions, such as, photo-electric emission stimulated by the ultra-violet radiation, collisional charging by electrons and ions, disruption and secondary emission due to the Maxwellian stress, etc. [8–12].

It has been found that the presence of static charged dust grains modifies the existing plasma wave spectra [13–20]. Bliokh and Yaroshenko [13] studied electrostatic waves in dusty plasmas and applied their results in interpreting spoke-like structures in Saturn's rings (revealed by Voyager space mission [21]). Angelis *et al.* [14] investigated the propagation of ion-acoustic waves in a dusty plasma, in which a spatial inhomogeneity is created by a distribution of immobile dust particles [22]. They [14] applied their results in interpreting the low frequency noise enhancement observed by the *Vega and Giotto* space probes in the dusty regions of Halley's comet [23].

On the other hand, it has been shown both theoretically [24–34] and experimentally [35, 36] that the dust charge dynamics introduces different new eigenmodes, such as dust-acoustic mode, dust-ion-acoustic mode, dust-drift mode, lower-hybrid mode, dust-cyclotron mode, etc. These collective processes or wave phenomena in a dusty plasma (containing extremely massive dust grains) can be studied in either of the three possible regimes, namely,

(i) the electromagnetic force is much greater than the gravitational force,
(ii) the electromagnetic force is of the same order of the magnitude as the gravitational force, and
(iii) the gravitational force is much greater than the electromagnetic force.

The case (i) corresponds to usual laboratory plasma situations where Coulombic interaction is primary responsible for the plasma dielectric behavior. The case (ii) corresponds to planetary atmospheres and interstellar media [3, 6, 37–39] where the thickness of the Jovian ring, spoke formation in Saturn's rings, etc. are thought to be due to the balance of these two forces. The case (iii) generally corresponds to astrophysical plasmas where the formation of large-scale structure is attributed to gravitational condensation [40].

[a] e-mail: am@egal.tp4.ruhr-uni-bochum.de

Most of these studies [24–34] on these new modes (associated with the dynamics of extremely massive dust grains) are concerned with situation (i), but not with cases (ii) and (iii). A number of investigations [41–45] have been made of dust-acoustic waves in a self-gravitating dusty plasma system. Pandey *et al.* [42], Mahanta *et al.* [43], and Mamun [44] have studied the effect of the gravitational field on dust-acoustic waves by ignoring the ion dynamics, whereas Avinash and Shukla [41] and Verheest *et al.* [45] have investigated dust-acoustic waves in a self-gravitating unmagnetized dusty plasma, taking into account the dynamics of dust grains and ions. The present work has considered a self-gravitating magnetized two fluid dusty plasma system and investigated ultra-low-frequency dust-electrostatic and dust-electromagnetic modes, namely, dust-cyclotron mode, dust-lower-hybrid mode, and dust-magnetosonic mode, propagating perpendicular to the external magnetic field.

The paper is organized as follows. The basic equations governing our dusty plasma system is presented in Section 2. A general dispersion relation for electrostatic or electromagnetic waves, associated with the dynamics of dust grains and ions, in a self-gravitating, warm, magnetized dusty plasma system is derived and dispersion properties of different ultra-low-frequency dust-modes, namely, dust-cyclotron mode, dust-lower-hybrid mode, and dust-magnetosonic mode, are studied in Section 3. Finally, a brief discussion is given in Section 4.

2 Governing equations

We consider a two-component, self-gravitating, warm, magnetized dusty plasma system consisting of negatively charged (extremely massive) dust grains and positively charged ions. Thus, at equilibrium we have $Z_\mathrm{i} n_{\mathrm{i}0} = Z_\mathrm{d} n_{\mathrm{d}0}$, where $n_{\mathrm{d}0}$ ($n_{\mathrm{i}0}$) is the equilibrium dust grain (ion) number density and Z_d (Z_i) is the number of electrons (protons) residing in a dust grain (ion). This plasma system is assumed to be immersed in an external static magnetic field. It has also been assumed here that the electron number density is highly depleted due to the attachment of all most all electrons to the surface of the extremely massive dust grains. This model is relevant to planetary ring-systems (*e.g.*, Saturn's F-ring [3, 26, 30]) and laboratory experiments [35, 36]. The macroscopic state of this self-gravitating, warm, magnetized dusty plasma system may be described by

$$\frac{\partial N_s}{\partial t} + \nabla\cdot(N_s\mathbf{U_s}) = 0, \tag{1}$$

$$\left(\frac{\partial}{\partial t} + \mathbf{U}_s\cdot\nabla\right)\mathbf{U_s} = \frac{q_s}{m_s}\left(\mathbf{E} + \frac{1}{c}\mathbf{U}_s\times\mathbf{B}\right) - \nabla\Psi - \frac{1}{N_s m_s}\nabla P_s, \tag{2}$$

$$\nabla\cdot\mathbf{E} = 4\pi\sum_s q_s N_s, \tag{3}$$

$$\nabla^2\Psi = 4\pi G\sum_s m_s N_s, \tag{4}$$

$$\mathbf{J} = \sum_s q_s N_s \mathbf{U}_s, \tag{5}$$

$$\nabla\times\mathbf{E} = -\frac{1}{c}\frac{\partial\mathbf{B}}{\partial t}, \tag{6}$$

$$\nabla\times\mathbf{B} = \frac{4\pi}{c}\mathbf{J} + \frac{1}{c}\frac{\partial\mathbf{E}}{\partial t}, \tag{7}$$

where $s = (\mathrm{i}, \mathrm{d})$ denotes the species, namely, ion and dust grain; m_s, q_s, and N_s are, respectively, mass, charge, and number density of the species s; $\mathbf{U}_s$ is the hydrodynamic velocity, $P_s = \gamma_s N_s k_\mathrm{B} T_s$, with $k_\mathrm{B} T_s$ being the thermal energy and γ_s being the adiabatic constant; $\mathbf{E}$ is the electric field and $\mathbf{B}$ is the magnetic field; G is the universal gravitational constant; $\mathbf{J}$ is the plasma current; c is the speed of light in vacuum.

3 Ultra-low-frequency dust-modes

We are interested in looking at a general low-frequency dust-mode (ω, $\mathbf{k}$), which may be electrostatic or electromagnetic, propagating perpendicular to the external magnetic field $\mathbf{B}_0$. We assume that the external magnetic field $\mathbf{B}_0$ is along the z-axis, *i.e.*, $\mathbf{B}_0 \parallel \hat{\mathbf{z}}$, and the propagation vector $\mathbf{k}$ is along the y-axis, *i.e.*, $\mathbf{k} \parallel \hat{\mathbf{y}}$. To study such a low-frequency dust-mode in a self-gravitating, warm, magnetized dusty plasma, we shall carry out a normal mode analysis. We first express our dependent variables N_s, U_s, $\mathbf{E}$, $\mathbf{B}$, Ψ, and $\mathbf{J}$ in terms of their equilibrium and perturbed parts as

$$\left.\begin{aligned} N_s &= n_{s0} + n_s\\ \mathbf{U}_s &= 0 + \mathbf{u}_s\\ \mathbf{E} &= 0 + \mathbf{E}_1\\ \mathbf{B} &= \mathbf{B}_0 + \mathbf{B}_1\\ \Psi &= 0 + \Psi_1\\ \mathbf{J} &= 0 + \mathbf{J}_1 \end{aligned}\right\}. \tag{8}$$

Then, using these equations, we linearize our basic equations to a first-order approximation and express them as

$$\frac{\partial n_s}{\partial t} + n_{s0}(\nabla\cdot\mathbf{u_s}) = 0, \tag{9}$$

$$\frac{\partial\mathbf{u}_s}{\partial t} = \frac{q_s}{m_s}(\mathbf{E}_1 + \frac{1}{c}\mathbf{u}_s\times\mathbf{B_0}) - \nabla\Psi_1 - \frac{v_{ts}^2}{n_{0s}}\nabla n_s, \tag{10}$$

$$\nabla\cdot\mathbf{E}_1 = 4\pi\sum_s q_s n_s, \tag{11}$$

$$\nabla^2\Psi_1 = 4\pi G\sum_s m_s n_s, \tag{12}$$

$$\mathbf{J}_1 = \sum_s q_s n_{s0} \mathbf{u}_s, \tag{13}$$

$$\nabla \times \mathbf{E}_1 = -\frac{1}{c}\frac{\partial \mathbf{B}_1}{\partial t}, \tag{14}$$

$$\nabla \times \mathbf{B}_1 = \frac{4\pi}{c}\mathbf{J}_1 + \frac{1}{c}\frac{\partial \mathbf{E_1}}{\partial t}, \tag{15}$$

where $v_{ts} = (\gamma_s k_{\rm B} T_s/m_s)^{1/2}$. Now, performing Fourier transformation of equations (9–12) and using them, one can obtain x, y, and z-components of ion and dust fluid velocities. Substituting these velocity components into equation (13), we can express this equation in the form

$$\mathbf{J}_1 = \boldsymbol{\sigma} \cdot \mathbf{E}_1, \tag{16}$$

where $\boldsymbol{\sigma}$ is the conductivity tensor, different elements of which are given by

$$\begin{aligned}
\sigma_{xx} &= \frac{{\rm i}\omega}{4\pi}\left[\frac{\omega_{\rm pd}^2}{\omega^2}\left(1+\frac{\omega_{\rm cd}^2}{\alpha_{\rm d}\beta\omega^2}\left[1-\frac{1}{\alpha_{\rm i}}\left(\frac{Z_{\rm i}m_{\rm d}}{Z_{\rm d}m_{\rm i}}\right)^2\frac{\omega_{\rm Ji}^2}{\omega^2}\right]\right)\right.\\
&\quad\left.+\frac{\omega_{\rm pi}^2}{\omega^2}\left(1+\frac{\omega_{\rm ci}^2}{\alpha_{\rm i}\beta\omega^2}\left[1-\frac{1}{\alpha_{\rm d}}\left(\frac{Z_{\rm d}m_{\rm i}}{Z_{\rm i}m_{\rm d}}\right)^2\frac{\omega_{\rm Jd}^2}{\omega^2}\right]\right)\right],\\
\sigma_{xy} &= \frac{\omega}{4\pi}\left[\frac{\omega_{\rm pd}^2\omega_{\rm cd}}{\alpha_{\rm d}\beta\omega^3}\left[1+\frac{1}{\alpha_{\rm i}}\left(\frac{Z_{\rm i}m_{\rm d}}{Z_{\rm d}m_{\rm i}}\right)\frac{\omega_{\rm Ji}^2}{\omega^2}\right]\right.\\
&\quad\left.-\frac{\omega_{\rm pi}^2\omega_{\rm ci}}{\alpha_{\rm i}\beta\omega^3}\left[1+\frac{1}{\alpha_{\rm d}}\left(\frac{Z_{\rm d}m_{\rm i}}{Z_{\rm i}m_{\rm d}}\right)\frac{\omega_{\rm Jd}^2}{\omega^2}\right]\right],\\
\sigma_{xz} &= \sigma_{zx} = 0,\\
\sigma_{yx} &= -\frac{\omega}{4\pi}\left[\frac{\omega_{\rm pd}^2\omega_{\rm cd}}{\alpha_{\rm d}\beta\omega^3}\left[1-\frac{1}{\alpha_{\rm i}}\left(\frac{Z_{\rm i}m_{\rm d}}{Z_{\rm d}m_{\rm i}}\right)^2\frac{\omega_{\rm Ji}^2}{\omega^2}\right]\right.\\
&\quad\left.-\frac{\omega_{\rm pi}^2\omega_{\rm ci}}{\alpha_{\rm i}\beta\omega^3}\left[1-\frac{1}{\alpha_{\rm d}}\left(\frac{Z_{\rm d}m_{\rm i}}{Z_{\rm i}m_{\rm d}}\right)^2\frac{\omega_{\rm Jd}^2}{\omega^2}\right]\right],\\
\sigma_{yy} &= \frac{{\rm i}\omega}{4\pi\beta}\left[\frac{\omega_{\rm pd}^2}{\alpha_{\rm d}\omega^2}\left[1+\frac{1}{\alpha_{\rm i}}\left(\frac{Z_{\rm i}m_{\rm d}}{Z_{\rm d}m_{\rm i}}\right)^2\frac{\omega_{\rm Ji}^2}{\omega^2}\right]\right.\\
&\quad\left.+\frac{\omega_{\rm pi}^2}{\alpha_{\rm i}\omega^2}\left[1+\frac{1}{\alpha_{\rm d}}\left(\frac{Z_{\rm d}m_{\rm i}}{Z_{\rm i}m_{\rm d}}\right)^2\frac{\omega_{\rm Jd}^2}{\omega^2}\right]\right],\\
\sigma_{yz} &= \sigma_{zy} = 0,\\
\sigma_{zz} &= \frac{{\rm i}\omega}{4\pi}\left[\frac{\omega_{\rm pd}^2}{\omega^2}+\frac{\omega_{\rm pi}^2}{\omega^2}\right],
\end{aligned} \tag{17}$$

with

$$\begin{aligned}
\alpha_s &= 1-\frac{\omega_{\rm cs}^2}{\omega^2}+\frac{\omega_{{\rm J}s}^2}{\omega^2}-\frac{k^2v_{ts}^2}{\omega^2},\\
\beta &= 1-\frac{\omega_{\rm Jd}^2\omega_{\rm Ji}^2}{\alpha_{\rm d}\alpha_{\rm i}\omega^4},\\
\omega_{{\rm p}s} &= \sqrt{4\pi n_{s0}Z_s^2e^2/m_s},\\
\omega_{{\rm J}s} &= \sqrt{4\pi G m_s n_{s0}}.\\
\omega_{{\rm c}s} &= \frac{Z_s e B_0}{m_s c}\,.
\end{aligned} \tag{18}$$

Now, using equations (14–16) one can obtain a general dispersion relation

$$\left(1-\frac{c^2k^2}{\omega^2}\right)\boldsymbol{I}+\frac{c^2}{\omega^2}\mathbf{k}\cdot\mathbf{k}+\frac{4\pi{\rm i}}{\omega}\boldsymbol{\sigma}=0, \tag{19}$$

where $\boldsymbol{I}$ is a unit tensor of rank 3. This is the general dispersion relation for any electrostatic or electromagnetic mode, propagating perpendicular to the external magnetic field, in a self-gravitating, warm, magnetized dusty plasma. However, our present interest is to study different low-frequency modes (associated with the dynamics of dust grains and ions), namely, dust-cyclotron mode, dust-lower-hybrid mode, and dust-magnetosonic mode. The first two are electrostatic ($\mathbf{k} \parallel \mathbf{E}_1$, *i.e*, $E_{1x} = E_{1z} = 0$) and the last one is electromagnetic ($\mathbf{k} \perp \mathbf{E}_1$, *i.e*, $E_{1y} = 0$). We now study these modes in more details.

3.1 Dust-cyclotron mode

To study dust-cyclotron mode (where $\mathbf{k} \parallel \mathbf{E}_1$, *i.e.*, $E_{1x} = E_{1z} = 0$) one can use $\sigma_{yx} \to 0$ and $\omega_{\rm Ji}, \omega_{\rm ci} \ll kv_{\rm ti}$. These approximations reduce the general dispersion relation to a simple form

$$\begin{aligned}
\omega^2 &= \omega_{\rm cd}^2 + k^2v_{\rm td}^2 + \frac{k^2C_{\rm d}^2}{1+k^2\lambda_{\rm Di}^2}\\
&\quad -\omega_{\rm Jd}^2\left[1+\left(\frac{Z_{\rm d}m_{\rm i}}{Z_{\rm i}m_{\rm d}}\right)\left(\frac{1}{1+k^2\lambda_{\rm Di}^2}\right)\right]\\
&\quad -\frac{\omega_{\rm Ji}^2}{1+k^2\lambda_{\rm Di}^2}\left[1+G\left(\frac{m_{\rm i}m_{\rm d}}{Z_{\rm i}Z_{\rm d}e^2}\right)\right],
\end{aligned} \tag{20}$$

where $C_{\rm d} = (\gamma_{\rm i} Z_{\rm d} k_{\rm B} T_{\rm i}/Z_{\rm i} m_{\rm d})^{1/2}$ and $\lambda_{{\rm D}s} = (\gamma_s k_{\rm B} T_s/4\pi n_{s0} Z_s^2 e^2)^{1/2}$. This equation represents the dispersion relation for the dust-cyclotron mode, in which the effects of self-gravitational field (acting on both dust particles and ions), thermal pressures of dust and ion fluids, and ion dynamics are included. If we consider unmagnetized case and neglect the effects of the self-gravitating field, ion dynamics and dust fluid temperature (*i.e.* $\omega_{\rm cd} \to 0$, $\omega_{\rm Jd,i} \to 0$, $k^2\lambda_{\rm Di}^2 \ll 1$, and $v_{\rm td} \to 0$), this becomes the dispersion relation for the dust-acoustic mode studied by Rao *et al.* [24]. On the other hand, if we neglect effects of external magnetic field and dust fluid temperature, but not of the self-gravitational field, our dispersion relation reduces to that obtained by Pandey *et al.* [42] when ion dynamics is neglected and to that by Verheest *et al.* [45] when ion dynamics is taken into account.

It is shown from our dispersion relation for the dust-cyclotron mode that due to the effect of the self-gravitational force acting on dust grains and ions, this mode becomes unstable if

$$\begin{aligned}
\left(\omega_{\rm cd}^2 + k^2v_{\rm td}^2 + \delta k^2 C_{\rm d}^2\right) &< \left(\omega_{\rm Jd}^2\left[1+\delta\left(\frac{Z_{\rm d}m_{\rm i}}{Z_{\rm i}m_{\rm d}}\right)\right]\right.\\
&\quad\left.+\delta\omega_{\rm Ji}^2\left[1+G\left(\frac{m_{\rm i}m_{\rm d}}{Z_{\rm i}Z_{\rm d}e^2}\right)\right]\right),
\end{aligned} \tag{21}$$

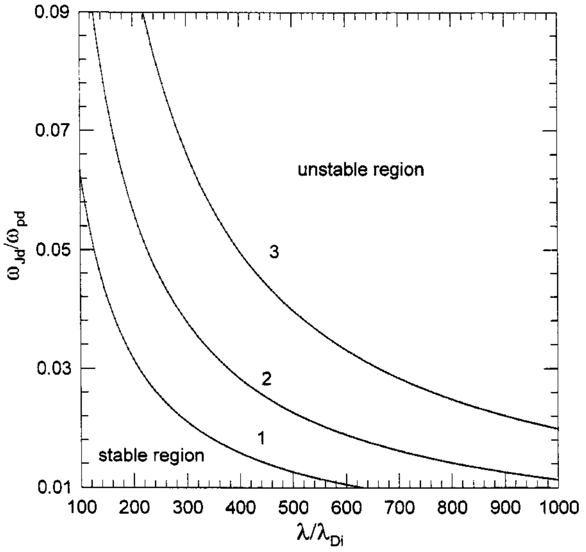

Fig. 1. $S_a = 0$ curves showing stable and unstable regions depending on corresponding values of ω_{Jd}/ω_{pd} and λ/λ_{Di} for $V_{Ad}/c = 1.0 \times 10^{-5}$ (curve 1), $V_{Ad}/c = 2.0 \times 10^{-5}$ (curve 2), and $V_{Ad}/c = 3 \times 10^{-5}$ (curve 3).

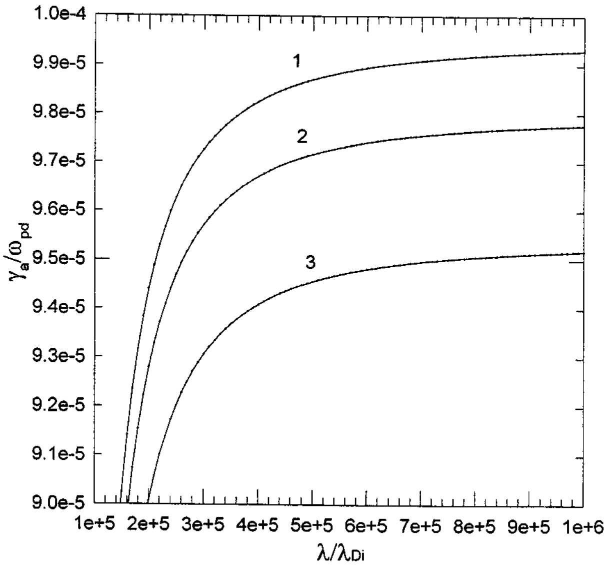

Fig. 2. Variation of the normalized growth rate (γ_a/ω_{pd}) of the unstable dust-cyclotron mode with the normalized wavelength λ/λ_{Di} for $\omega_{Jd}/\omega_{pd} = 10^{-5}$, $V_{Ad}/c = 1.0\times10^{-5}$ (curve 1), $V_{Ad}/c = 2.0\times10^{-5}$ (curve 2), and $V_{Ad}/c = 3.0\times10^{-5}$ (curve 3).

where $\delta = 1/(1+k^2{\lambda_{Di}}^2)$. The criterion for this instability (known as gravitational instability), for $k^2\lambda_{Di}^2 \ll 1$ and $(Z_d m_i/Z_i m_d) \ll 1$, can be simplified as

$$S_a > 0, \tag{22}$$

$$S_a \simeq \frac{\omega_{Jd}^2}{\omega_{pd}^2} - \frac{V_{Ad}^2}{c^2} - \left(\frac{2\pi}{\lambda/\lambda_{Di}}\right)^2, \tag{23}$$

where $V_{Ad} = B_0/\sqrt{4\pi n_{d0} m_d}$, and the growth rate γ_a of this unstable mode is given by

$$\gamma_a \simeq \sqrt{S_a}. \tag{24}$$

In order to have some numerical appreciations of our results we have plotted $S_a = 0$ curves (showing stable and unstable regions) and obtained numerical values of the growth rate γ_a for different values of V_{Ad}/c. These are displayed in Figures 1–3 . Here, we choose $\lambda/\lambda_{Di} \simeq 10^5$–$10^6$, $\omega_{Jd}/\omega_{pd} \simeq 10^{-5}$–$10^{-6}$, $V_{Ad}/c = 1.0 \times 10^{-5}$ (curve 1), $V_{Ad}/c = 2.0 \times 10^{-5}$ (curve 2), $V_{Ad}/c = 3.0 \times 10^{-5}$ (curve 3). These values correspond to usual space dusty plasma parameters [3, 6, 46–48] of interests, *viz.* $n_{d0} \simeq 10^{-7}$–10 cm^{-3}, $Z_d \simeq 10$–10^4, $T_i \simeq T_d \simeq 10^4$–$10^6$ K, $m_d \simeq 10^{-12}$–10^{-7} gm, $B_0 \simeq 10^{-3}$–10 G, etc.

It is now obvious from both of our analytical and numerical calculations (Fig. 1) that the dust-cyclotron mode may become unstable due to the effect of the self-gravitational force acting on dust grains. It is also shown that the effects of the external magnetic field and the thermal pressures of both dust and ion fluids try to stabilize this dust-cyclotron mode and counter the gravitational condensation of the dust grains. It is observed from Figures 2 and 3 that the growth rate γ_a of this unstable dust-cyclotron mode increases with increasing the values of ω_{Jd}/ω_{pd} and λ/λ_{Di}, but decreases with increasing the value of V_{Ad}/c.

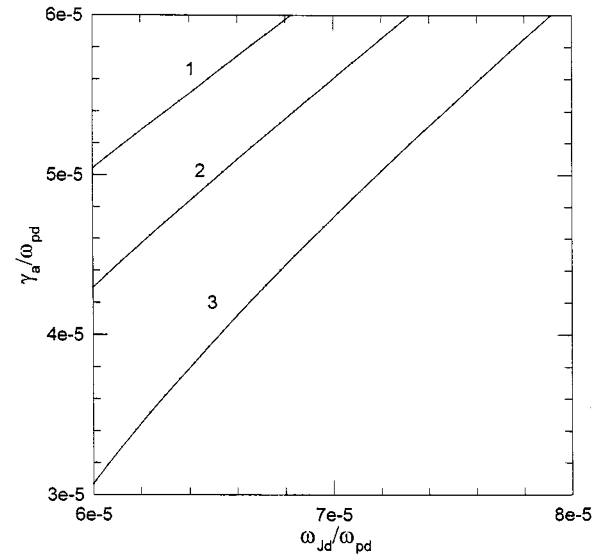

Fig. 3. Variation of the normalized growth rate (γ_a/ω_{pd}) of the unstable dust-cyclotron mode with the normalized Jeans frequency (ω_{Jd}/ω_{pd}) for $\lambda/\lambda_{Di} = 5.0 \times 10^5$, $V_{Ad}/c = 1.0\times10^{-5}$ (curve 1), $V_{Ad}/c = 2.0\times10^{-5}$ (curve 2), and $V_{Ad}/c = 3.0\times10^{-5}$ (curve 3).

3.2 Dust-lower-hybrid mode

To examine dust-lower-hybrid mode (where $\mathbf{k} \parallel \mathbf{E}_1$, *i.e.*, $E_{1x} = E_{1z} = 0$) we can use $\sigma_{yx} \to 0$, $\omega_{cd} < \omega < \omega_{ci}$, and ω_{Ji}, $kv_{ti} \ll \omega_{ci}$. These approximations reduce the general

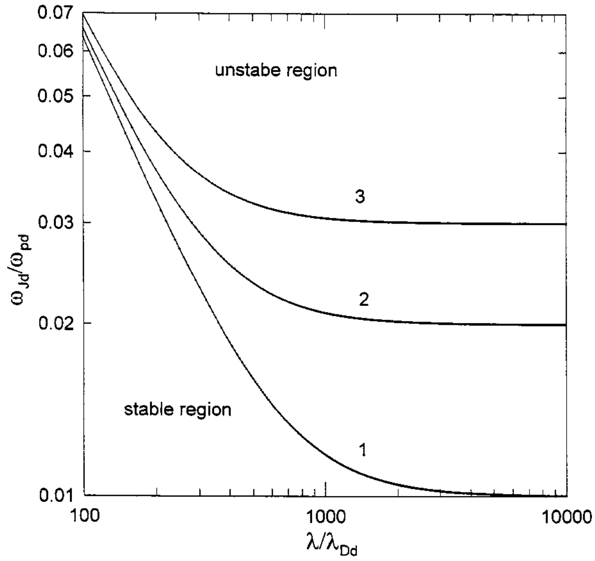

Fig. 4. $S_\mathrm{b} = 0$ curves showing stable and unstable regions depending on corresponding values of $\omega_\mathrm{Jd}/\omega_\mathrm{pd}$ and $\lambda/\lambda_\mathrm{Dd}$ for $V_\mathrm{Ai}/c = 0.01$ (curve 1), $V_\mathrm{Ai}/c = 0.02$ (curve 2), and $V_\mathrm{Ai}/c = 0.03$ (curve 3).

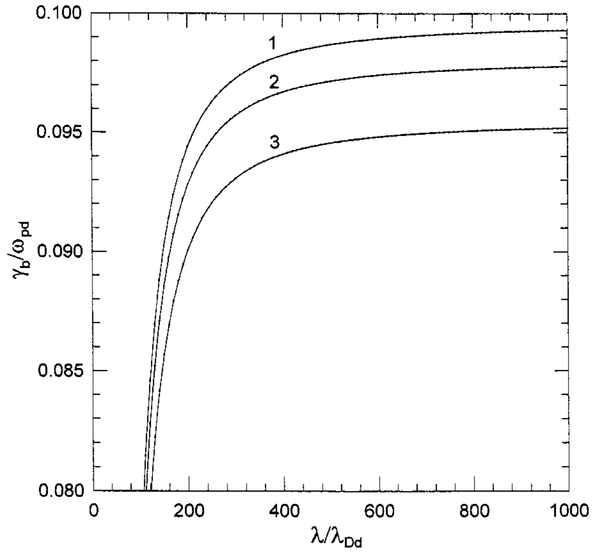

Fig. 5. Variation of the normalized growth rate ($\gamma_\mathrm{b}/\omega_\mathrm{pd}$) of the unstable dust-lower-hybrid mode with the normalized wavelength $\lambda/\lambda_\mathrm{Dd}$ for $\omega_\mathrm{Jd}/\omega_\mathrm{pd} = 0.10$, $V_\mathrm{Ai}/c = 0.01$ (curve 1), $V_\mathrm{Ai}/c = 0.02$ (curve 2), and $V_\mathrm{Ai}/c = 0.03$ (curve 3).

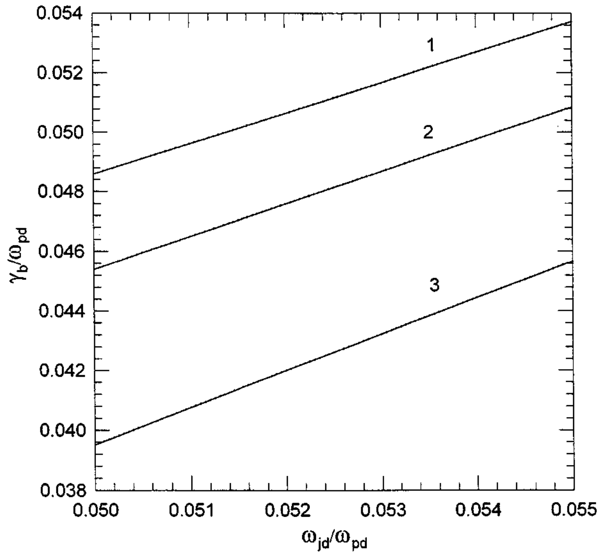

Fig. 6. Variation of the normalized growth rate ($\gamma_\mathrm{b}/\omega_\mathrm{pd}$) of the unstable dust-lower-hybrid mode with the normalized Jeans frequency ($\omega_\mathrm{Jd}/\omega_\mathrm{pd}$) for $\lambda/\lambda_\mathrm{Dd} = 1.0 \times 10^3$, $V_\mathrm{Ai}/c = 0.01$ (curve 1), $V_\mathrm{Ai}/c = 0.02$ (curve 2), and $V_\mathrm{Ai}/c = 0.03$ (curve 3).

dispersion relation to a simple form

$$\omega^2 = \omega_\mathrm{cd}\omega_\mathrm{ci}\left(1 + \frac{\omega_\mathrm{cd}\omega_\mathrm{ci}}{\omega_\mathrm{pd}^2}\right)^{-1} + k^2 v_\mathrm{td}^2 - \omega_\mathrm{Jd}^2\left[1 + \frac{Z_\mathrm{d} m_\mathrm{i}}{Z_\mathrm{i} m_\mathrm{d}}\left(1 + \frac{\omega_\mathrm{cd}\omega_\mathrm{ci}}{\omega_\mathrm{pd}^2}\right)^{-1}\right] - \omega_\mathrm{Ji}^2\left(1 + \frac{\omega_\mathrm{cd}\omega_\mathrm{ci}}{\omega_\mathrm{pd}^2}\right)^{-1}\left[1 + G\left(\frac{m_\mathrm{i} m_\mathrm{d}}{Z_\mathrm{i} Z_\mathrm{d} e^2}\right)\right]. \quad (25)$$

This equation represents the dispersion relation for the dust-lower-hybrid mode where the effects of self-gravitational field (acting on both dust particles and ions), thermal pressures of dust and ion fluids are included. It is shown from this dispersion relation that the effects of the self-gravitational field and dust fluid temperature modify this dust-lower-hybrid mode significantly, and that due to the effect of this self-gravitational field, this dust-lower-hybrid mode becomes unstable if

$$\left(\mu\omega_\mathrm{cd}\omega_\mathrm{ci} + k^2 v_\mathrm{td}^2\right) < \left(\omega_\mathrm{Jd}^2\left[1 + \mu\left(\frac{Z_\mathrm{d} m_\mathrm{i}}{Z_\mathrm{i} m_\mathrm{d}}\right)\right] + \mu\omega_\mathrm{Ji}^2\left[1 + G\left(\frac{m_\mathrm{i} m_\mathrm{d}}{Z_\mathrm{i} Z_\mathrm{d} e^2}\right)\right]\right), \quad (26)$$

where $\mu = (1 + \omega_\mathrm{cd}\omega_\mathrm{ci}/\omega_\mathrm{pd}^2)^{-1}$. The criterion for this instability (known as gravitational instability), for $\omega_\mathrm{ci}\omega_\mathrm{cd}/\omega_\mathrm{pd}^2 \ll 1$ and $Z_\mathrm{d} m_\mathrm{i}/Z_\mathrm{i} m_\mathrm{d} \ll 1$, can be simplified as

$$S_\mathrm{b} > 0, \quad (27)$$

$$S_\mathrm{b} \simeq \frac{\omega_\mathrm{Jd}^2}{\omega_\mathrm{pd}^2} - \frac{V_\mathrm{Ai}^2}{c^2} - \left(\frac{2\pi}{\lambda/\lambda_\mathrm{Dd}}\right)^2, \quad (28)$$

where $V_\mathrm{Ai} = B_0/\sqrt{4\pi n_{\mathrm{i}0} m_\mathrm{i}}$, and the growth rate γ_b of this unstable mode is given by

$$\gamma_\mathrm{b} = \sqrt{S_\mathrm{b}}. \quad (29)$$

To have some numerical appreciations of our results we have plotted $S_\mathrm{b} = 0$ curves (showing stable and unstable regions) and obtained numerical values of the growth rate γ_b for different values of V_Ai/c. These are shown in Figures 4–6. Here, we choose $\lambda/\lambda_\mathrm{Dd} = 10^2$–$10^4$, $\omega_\mathrm{Jd}/\omega_\mathrm{pd} \simeq 0.01$–$0.1$, $V_\mathrm{Ai}/c = 0.01$ (curve 1), $V_\mathrm{Ai}/c = 0.02$ (curve 2), $V_\mathrm{Ai}/c = 0.03$ (curve 3). These values also correspond to usual space dusty plasma parameters given in our previous case.

It is now obvious from both of our analytical and numerical calculations (Fig. 4) that the effect of the self-gravitational field and the increase in the wavelength of the mode try to destabilize the dust-lower-hybrid mode, whereas the effects of the external magnetic field and the thermal pressure of the dust fluid try to stabilize this mode and counter the gravitational condensation of the dust grains. It is also shown from Figures 5 and 6 that the growth rate γ_b of this unstable dust-lower-hybrid mode increases with increasing the values of ω_{Jd}/ω_{pd} and λ/λ_{Dd}, but decreases with increasing the value of V_{Ai}/c.

3.3 Dust-magnetosonic mode

To examine dust-magnetosonic mode (where $\mathbf{k} \perp \mathbf{E}_1$, *i.e.*, $E_{1y} = 0$) we use $\omega \ll \omega_{cd}$ and $k^2 v_{ti}^2 \gg (\omega_{Jd}^2 + \omega_{Ji}^2)$. These approximations reduce the general dispersion relation to

$$\omega^2 = \frac{1}{1 + V_{Ad}^2/c^2} \times \left[k^2 V_{Ad}^2 + k^2 C_d^2 + k^2 v_{td}^2 - (\omega_{Jd}^2 + \omega_{Ji}^2)\right]. \quad (30)$$

This is the dispersion relation for an extremely low-frequency dust-electromagnetic mode where effects of self-gravitating field, magnetic pressures, and dust and ion thermal pressures are included. If we neglect the effects of the self-gravitating field and dust fluid temperature, this dispersion relation, for $V_{Ad} \ll c$, becomes

$$\frac{\omega^2}{k^2} \simeq V_{Ad}^2 + C_d^2 = \frac{B_0^2/4\pi + \gamma_i n_{i0} k_B T_i}{n_{d0} m_d}. \quad (31)$$

This means that this is an extremely low phase velocity electromagnetic mode, propagating perpendicular to the external magnetic field, where the dust mass density provides the inertia and the sum of magnetic pressure ($B_0^2/4\pi$) and ion thermal pressure ($\gamma_i n_{i0} k_B T_i$) gives rise to the restoring force. Thus, we can call this mode the dust-magnetosonic mode. It is seen from the general dispersion relation for this ultra-low-frequency magnetosonic mode that this mode is significantly modified by the effects of self-gravitational field and dust fluid temperature. It is also found that due to the effect of the self-gravitational field, this mode becomes unstable if

$$S_c > 0, \quad (32)$$

$$S_c \simeq \frac{\omega_{Jd}^2}{\omega_{pd}^2} - \left(\frac{2\pi}{\lambda/\lambda_{Di}}\right)^2 \left(1 + \frac{V_{Ad}^2}{C_d^2}\right). \quad (33)$$

The growth rate γ_c of the mode, satisfying this instability criterion, is given by

$$\gamma_c \simeq \sqrt{S_c}. \quad (34)$$

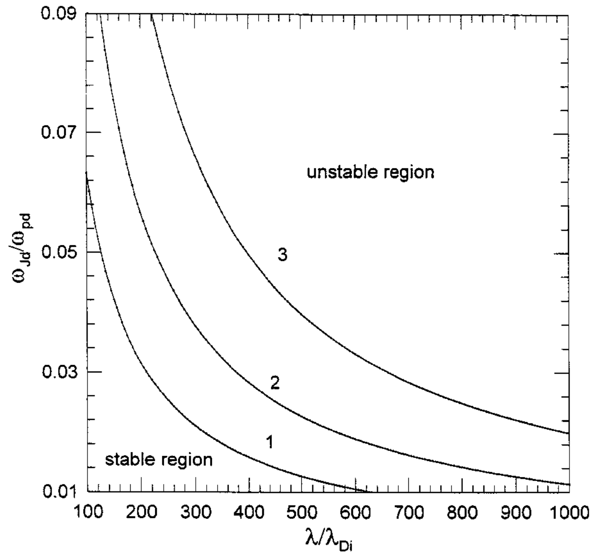

Fig. 7. $S_c = 0$ curves showing stable and unstable regions depending on corresponding values of ω_{Jd}/ω_{pd} and λ/λ_{Di} for $V_{Ad}/C_d = 1$ (curve 1), $V_{Ad}/C_d = 2$ (curve 2), and $V_{Ad}/C_d = 3$ (curve 3).

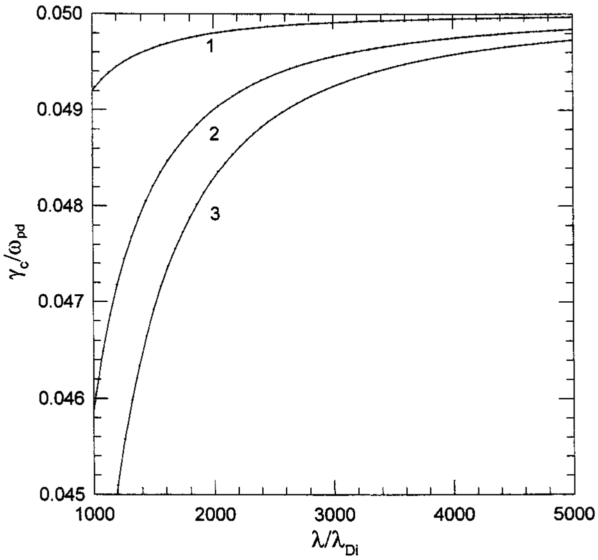

Fig. 8. Variation of the normalized growth rate (γ_c/ω_{pd}) of the unstable dust-magnetosonic mode with the normalized wavelength λ/λ_{Di} for $\omega_{Jd}/\omega_{pd} = 0.05$, $V_{Ad}/C_d = 1$ (curve 1), $V_{Ad}/C_d = 2$ (curve 2), and $V_{Ad}/C_d = 3$ (curve 3).

Again, in order to have some numerical appreciations of our results we have plotted $S_c = 0$ curves (showing stable and unstable regions) and obtained numerical values of the growth rate γ_c for different values of V_{Ad}/C_d. These are displayed in Figures 7–9. Here, we choose $\lambda/\lambda_{Di} \simeq 10^2$–$10^3$, $\omega_{Jd}/\omega_{pd} \simeq 10^{-3}$–$10^{-4}$, $V_{Ad}/C_d = 1$ (curve 1), $V_{Ad}/C_d = 3$ (curve 2), $V_{Ad}/C_d = 4$ (curve 3). These values again correspond to usual space dusty plasma parameters mentioned in our earlier cases.

It is now obvious from both of our analytical and numerical calculations (Fig. 7) that the effect of

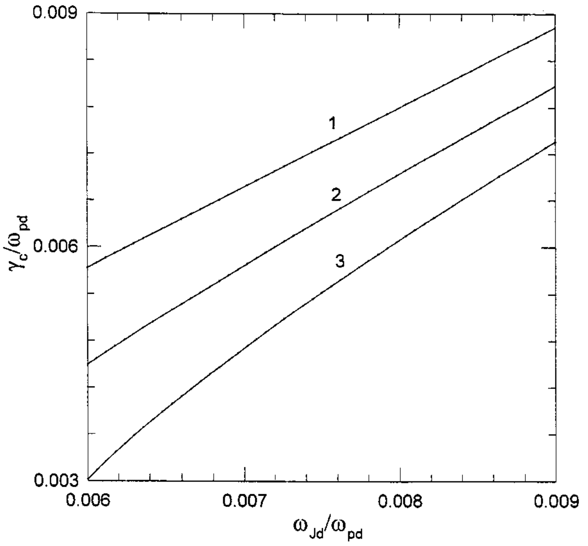

Fig. 9. Variation of the normalized growth rate ($\gamma_c/\omega_{\rm pd}$) of the unstable dust-magnetosonic mode with the normalized Jeans frequency ($\omega_{\rm Jd}/\omega_{\rm pd}$) for $\lambda/\lambda_{\rm Di} = 5.0 \times 10^3$, $V_{\rm Ad}/C_{\rm d} = 1$ (curve 1), $V_{\rm Ad}/C_{\rm d} = 2$ (curve 2), and $V_{\rm Ad}/C_{\rm d} = 3$ (curve 3).

the self-gravitational field and the increase in the wavelength of the mode try to destabilize this ultra-low-frequency dust-magnetosonic mode, whereas the effects of the external magnetic field and the thermal pressure of the dust fluid try to stabilize this mode and counter the gravitational condensation of the dust grains. It is also shown from Figures 8 and 9 that the growth rate γ_c of this unstable mode increases with increasing the values of $\omega_{\rm Jd}/\omega_{\rm pd}$ and $\lambda/\lambda_{\rm Di}$, but decreases with increasing the value of $V_{\rm Ad}/C_{\rm d}$.

4 Discussion

A self-consistent and general description of linear ultra-low-frequency dust-electrostatic and dust-electromagnetic waves (propagating perpendicular to the ambient magnetic field) in a self-gravitating, warm, magnetized, two-component dusty plasma has been presented. It is assumed here that the electron number density is highly depleted due to the attachment of all most all electrons to the surface of the extremely massive dust grains. This assumption is relevant to planetary ring-systems (*e.g.*, Saturn's F-ring [3,26,30]) and laboratory experiments [35,36]. The results, which are obtained from this theoretical investigation, may be pointed out as follows.

(i) It is found that a dusty plasma, containing negatively charged (extremely massive) dust grains and positively charged ions, may support different new ultra-low-frequency modes namely, dust-cyclotron mode, dust-lower-hybrid mode, and dust-magnetosonic mode, propagating perpendicular to the external magnetic field.

(ii) It is obvious from our dispersion relations for these new modes that the phase velocity of the dust-cyclotron mode is $Z_{\rm d}m_{\rm i}/Z_{\rm i}m_{\rm d}$ (whose value [33] may range from 10^{-6} to 10^{-12}) times smaller than that of the ion-cyclotron mode, whereas the phase velocity of the dust-lower-hybrid mode is $Z_{\rm d}m_{\rm e}/m_{\rm d}$ (where $m_{\rm e}$ is the mass of an electron) times smaller than that of the ion-lower-hybrid mode. The phase velocity of the dust-magnetosonic mode is also approximately $Z_{\rm d}m_{\rm i}/Z_{\rm i}m_{\rm d}$ times smaller than that of the ion-magnetosonic mode.

(iii) It is observed that the effect of the self-gravitational field, acting on both dust grains and ions, tries to make all these low-frequency modes (dust-cyclotron mode, dust-lower-hybrid mode, and dust-magnetosonic mode) unstable, whereas effects of the dust-temperature and the external magnetic field play stabilizing role, *i.e.*, try to make these modes stable and counter the gravitational condensation of the dust grains (Figs. 1, 4, and 7).

(iv) It is also shown from our numerical calculations (Figs. 2 and 3, 5 and 6, 8 and 9) that the growth rate of these low-frequency unstable modes (dust-cyclotron mode, dust-lower-hybrid mode, and dust-magnetosonic mode) increases with increasing the values of the gravitational force (*i.e.*, $m_{\rm d}$) and wavelength of the mode (λ), but decreases with increasing the value of the external magnetic field (B_0).

It should be mentioned here that for our numerical calculations we choose a wide range of values for each of our involved parameters which are, of course, typical for a number of space dusty plasma systems, particularly, for planetary ring systems (typical approximate plasma parameters [3, 6, 46–48] in planetary ring systems are $n_{\rm d0} \simeq 10^{-7}$–$1$ cm^{-3}, $Z_{\rm d} \simeq 10$–10^4, $T_{\rm i} \simeq T_{\rm d} \simeq 10^4$–$10^6$ K, $m_{\rm d} \simeq 10^{-12}$–$10^{-7}$ gm, $B_0 \simeq 10^{-3} - 10$ G, etc.) and cometary environments (typical approximate plasma parameters [3, 6, 46–48] in dust regions (tails) of Halley's comet are $n_{\rm d0} \simeq 10^{-7}$–$10^{-3}$ cm^{-3}, $Z_{\rm d} \simeq 10^4 - 10^5$, $T_{\rm i} \simeq T_{\rm d} \simeq 10^3$–$10^4$ K, $m_{\rm d} \simeq 10^{-12}$–$10^{-7}$ gm, $B_0 \simeq 10^{-3}$–0.1 G, etc.).

It may be stressed here that the results of the present investigation may be useful for understanding the electrostatic and electromagnetic disturbances in a number of astrophysical dusty plasma systems, such as, planetary ring systems (*viz.* Saturn's rings [3,13,21]), cometary environment (*viz.* Halley's comet [14,23]), interstellar medium [3], etc., where negatively charged dust particulates and positively charged ions are the major plasma species. These results are specially applicable to planetary ring systems, because the planetary magnetic field lines from a nearly aligned dipole (Jupiter, Saturn, etc.) are perpendicular to the equatorial plane in which the bulk of the ring material moves.

It may also be added here that the effects of inhomogeneities in plasma density and external magnetic field on these low-frequency electrostatic and electromagnetic perturbation modes, and their instabilities are also problems of great importance, but beyond the scope of the present work.

The authors would like to express his gratitude to Prof. P.K. Shukla, Prof. R.A. Cairns, and Prof. M. Salimullah, and Dr. Y. Hayashi for their stimulating influence and helpful discussions during the course of this work.

References

1. M. Horanyi, D.A. Mendis, Astrophys. J. **294**, 357 (1985).
2. M. Horanyi, D.A. Mendis, Astrophys. J. **307**, 800 (1986).
3. C.K. Goertz, Rev. Geophys. **27**, 271 (1989).
4. T.G. Northrop, Phys. Scripta **45**, 475 (1992).
5. D.A. Mendis, M. Rosenberg, IEEE Trans. Plasma Sci. **20**, 929 (1992).
6. D.A. Mendis, M. Rosenberg, Annu. Rev. Astron. Astrophys. **32**, 419 (1994).
7. F. Verheest, Space Sci. Rev. **77**, 267 (1996).
8. B. Feuerbacher, R.F. Willis, B. Fitton, Astrophys. J. **181**, 101 (1973).
9. H. Fechting, E. Grün, G.E. Morfill, Planet. Space Sci. **27**, 511 (1979).
10. O. Havnes, C.K. Goertz, G.E. Morfill, E. Grün, W. Ip, J. Geophys. Res. **92**, 2281 (1987).
11. M.S. Barnes, J.H. Keller, J.C. Forster, J.A. O'Neil, D.K. Coultas, Phys. Rev. Lett. **68**, 313 (1992).
12. B. Walch, M. Horanyi, S. Robertson, Phys. Rev. Lett. **75**, 838 (1995).
13. P.V. Bliokh, V.V. Yaroshenko, Sov. Astron. **29**, 330 (1985).
14. U. de Angelis, V. Formisano, M. Giordano, J. Plasma Phys. **40**, 399 (1988).
15. U. de Angelis, R. Bingham, V.N. Tsytovich, J. Plasma Phys. **42**, 445 (1989).
16. N. D'Angelo, Planet. Space Sci. **38**, 1143 (1990).
17. R. Bingham, U. de Angelis, V.N. Tsytovich, O. Havnes, Phys. Fluids B **3**, 811 (1991).
18. P.K. Shukla, L. Stenflo, Astrophys. Space Sci. **190**, 23 (1992).
19. U. de Angelis, A. Forlani, R. Bingham, P.K. Shukla, A. Ponomarev, V.N. Tsytovich, Phys. Plasmas **1**, 236 (1994).
20. P.K. Shukla, S.V. Vladimirov, Phys. Plasmas **2**, 3179 (1995).
21. B.A. Smith *et al.*, Science **215**, 504 (1982).
22. E.C. Whipple, T.G. Northrop, D.A. Mendis, J. Geophys. Res. **90**, 7405 (1985).
23. R. Grard *et al.*, Nature **321**, 290 (1986).
24. N.N. Rao, P.K. Shukla, M.Y. Yu, Planet. Space Sci. **38**, 543 (1990).
25. P.K. Shukla, M.Y. Yu, R. Bharuthram, J. Geophys. Res. **96**, 21343 (1991).
26. P.K. Shukla, V.P. Silin, Phys. Scripta **45**, 508 (1992).
27. P.K. Shukla, Phys. Scripta **45**, 504 (1992).
28. M. Rosenberg, Planet. Space Sci. **41**, 229 (1993).
29. F. Melandø, T.K. Aslaksen, O. Havnes, Planet. Space Sci. **41**, 321 (1993).
30. A.A. Mamun, R.A. Cairns, P.K. Shukla, Phys. Plasmas **3**, 702 (1996).
31. P.K. Shukla, H.U. Rahman, Planet. Space Sci. **46**, 541 (1998).
32. D. Winske, M.S. Murillo, M. Rosenberg, Phys. Rev. E **59**, 2263 (1999).
33. M. Salimullah, G.E. Morfill, Phys. Rev. E **59**, 2558 (1999).
34. A.A. Mamun, M. Salahuddin, M. Salimullah, Planet. Space Sci. **47**, 79 (1999).
35. A. Barkan, R.L. Merlino, N. D'Angelo, Phys. Plasmas **2**, 3563 (1995).
36. N. D'Angelo, J. Phys. D **28**, 1009 (1995).
37. H. Alfvén, D.A. Mendis, Adv. Space Res. **3**, 95 (1983).
38. W. Hartquist, O. Havnes, G.E. Morfill, Fund. Cosmic Phys. **15**, 107 (1992).
39. D.A. Mendis, H.L.F. Houpis, J.R. Hill, J. Geophys. Res. **87**, 3449 (1982).
40. J. Binney, S. Tremaine, *Galactic Dynamics* (Princeton University Press, 1988).
41. K. Avinash, P.K. Shukla, Phys. Lett. A **189**, 470 (1994).
42. B.P. Pandey, K. Avinash, C.B. Dwivedi, Phys. Rev. E **49**, 5599 (1994).
43. L. Mahanta, B.J. Saikia, B.P. Pandey, S. Bujarbarua, J. Plasma Phys. **55**, 401 (1996).
44. A.A. Mamun, Phys. Plasmas **5**, 3542 (1998).
45. F. Verheest, P.K. Shukla, N.N. Rao, P. Meuris, J. Plasma Phys. **58**, 163 (1997).
46. V.N. Tsytovich, G.E. Morfill, R. Bingham, U. de Angelis, Comm. Plasma Phys. Contr. Fusion **13**, 153 (1990).
47. U. de Angelis, Phys. Scripta **45**, 465 (1992).
48. M. Resenberg, in *The Physics of Dusty Plasmas*, edited by P.K. Shukla, D.A. Mendis, V.W. Chow (World Scientific, 1996), p. 129.